

Higher-order Dynamical Effects in Breakup Reactions of weakly bound nuclei

Henning Esbensen

Argonne National Laboratory, Argonne, Illinois, USA.

- Coulomb dissociation of weakly bound nuclei is dominated by E1 transitions and first-order perturbation theory is often used to extract the E1 strength from data ([Weizsäcker-Williams method, 1934.](#))
- We developed a semiclassical description to test this method - a collaboration with George and others, from 1995 to 2005.
- A further test is to infer the rate of the inverse radiative capture from the extracted E1 strength and compare it to direct capture measurements. Examples : ${}^8\text{B} \rightarrow {}^7\text{Be} + \text{p}$ and ${}^{15}\text{C} \rightarrow {}^{14}\text{C} + \text{n}$.
- Compare the semiclassical method to CDCC calculations.

Work supported by U.S. Department of Energy,
Office of Nuclear Physics



Semiclassical description of breakup reactions, *Esbensen, Bertsch & Bertulani*, NPA 581, 107 (1995).

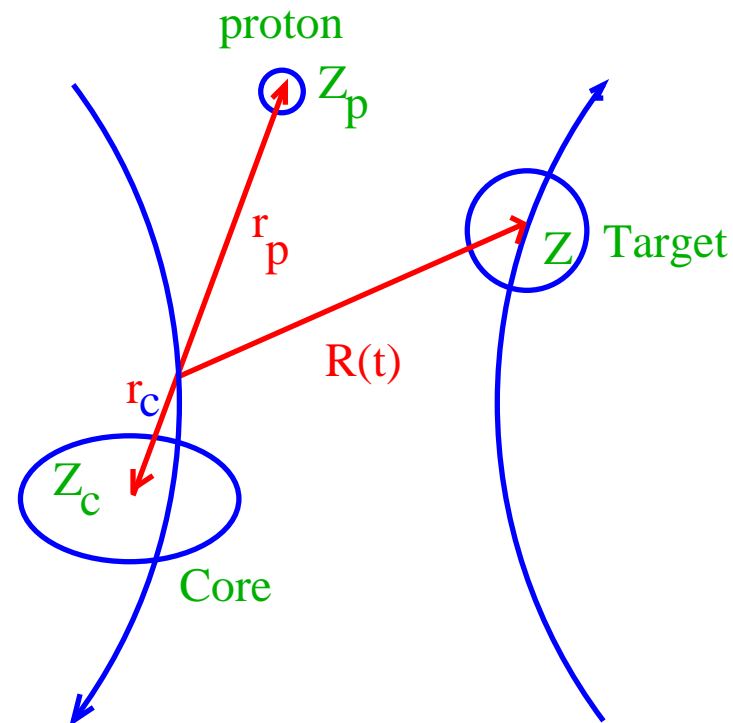
- Use classical Coulomb trajectories for the projectile-target motion.
- Solve time-dependent Schrödinger equation (TDSE) for the relative motion of a valence nucleon and the core in the **time-dependent field V_{ext} from a target nucleus**,

$$i\hbar \frac{d\Psi(\mathbf{r}, t)}{dt} = [H_0 + V_{ext}(\mathbf{r}, \mathbf{R}(t))] \Psi(\mathbf{r}, t).$$

H_0 is the intrinsic two-body Hamiltonian for a halo nucleus.

e. g., ${}^8\text{B} = {}^7\text{Be} + \text{p}$.

It is simulated by a simple Woods-Saxon well.



Propagator method

$$\Psi(t + \delta t) = \left[1 - \frac{\delta t}{2i\hbar} H_0\right]^{-1} \left[1 + \frac{\delta t}{2i\hbar} H_0\right] \left[1 + \frac{\delta t}{i\hbar} V_{\text{ext}}(t)\right] \Psi(t).$$

Kido-Yabana-Suzuki, PRC 53, 2296 (1996). (Other methods exist.)

Operator inversion: use the *Bonche-Koonin-Negele* TDHF method.

Expand wave function,

$$\Psi(\mathbf{r}, t) = \frac{1}{r} \sum_{ljm}^{L_{\text{max}}} u_{ljm}(r, t) |ljm\rangle.$$

Put the initial state on a radial grid: $r_{\text{max}} = 100$ fm in steps of 0.1 fm.

Evolve $\Psi(t)$ and stop before it reflects from the boundary at r_{max} .

Extract all information from the final wave function, $\Psi(t_f)$.

Coulomb plus nuclear potentials,

$$V_{ext}(\mathbf{r}, \mathbf{R}) = \frac{Z_p Z_T e^2}{|\mathbf{r}_p - \mathbf{R}|} + \frac{Z_c Z_T e^2}{|\mathbf{r}_c - \mathbf{R}|} + U_{pT} + U_{cT}.$$

$$\text{Multipole expansion : } \frac{1}{|\mathbf{r}_x - \mathbf{R}|} = \sum_{\lambda} \frac{r_x^{\lambda}}{R^{\lambda+1}} P_{\lambda}(\cos(\theta)).$$

The **far-field approximation** assumes that $r_x < R$:

$$\frac{1}{|\mathbf{r}_x - \mathbf{R}|} \approx \sum_{\lambda} \frac{r_x^{\lambda}}{R^{\lambda+1}} P_{\lambda}(\cos(\theta)).$$

It simplifies the analysis of CD data because:

$$\frac{d\sigma}{dE} = \Phi_{\lambda}(E) \frac{dB(E\lambda)}{dE}.$$

The far-field approx. is usually valid for the core-target interaction because $r_c \ll R$. It is therefore a good approx. for **neutron halo nuclei**. It breaks down at close collisions for **proton halo nuclei**, where $r_p > R$.

Coulomb dissociation of weakly bound nuclei is usually dominated by E1 transitions.

The E2 field from the core-target interaction is very weak ($\propto r_c^2/R^3$) because $r_c \ll R$. The E2 field can be ignored for **neutron halo nuclei**.

The E2 field from the proton-target interaction cannot be ignored. That complicates the Coulomb dissociation of **proton halo nuclei**.

Dynamic polarization of proton halo nuclei.

A first-order E1 transition to the continuum can interfere with a second-order process consisting of an E1 followed by an E2 transition

$$A_{\lambda=1} = A^{(1)}(E1) + A^{(2)}(E1, E2) + \dots$$

The excitation probability is

$$P_{\lambda=1} = |A^{(1)}(E1)|^2 + 2\text{Re}[A^{(1)}(E1)^* A^{(2)}(E1, E2)] + \dots$$

The **correction term** is of third order in the charge, **the Z^3 effect**.

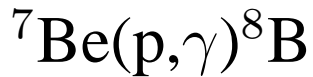
$$\text{Is } \sigma_{CD} = \sigma_{E1} + \sigma_{E1;E1,E2} + \sigma_{E2} + \sigma_{E2;E1,E1} + \dots \approx \sigma_{E1}?$$

Radiative Capture **RC** and Coulomb Dissociation **CD**

are closely related in the far-field approximation (*Baur-Bertulani-Rebel.*)

First-order Coul. Dissoc. (**CD**): $\frac{d\sigma^{(CD)}}{dE} = \Phi_\lambda(E) \frac{dB(E1)}{dE}$.

Radiative capture (**RC**): $\sigma_{E1}^{(RC)} \propto \frac{dB(E1)}{dE}$.



S-factor:

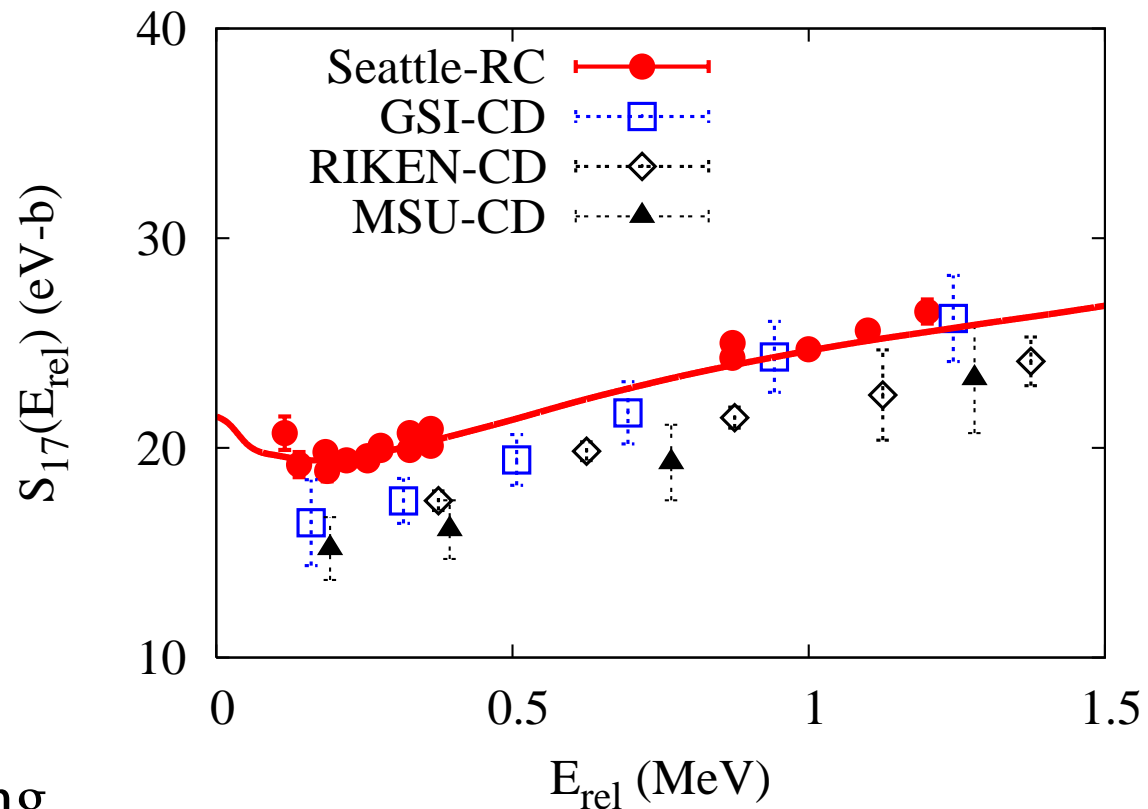
$$S_{17}(E_{rel}) = \sigma_{E1}^{(rc)} \times E_{rel} \exp(2\pi\eta).$$

A discrepancy $\approx 15\%$.

between **CD** and **RC**.

Can be reduced by using

the correct near-field/far-field **form factors** and include **E2 transitions**, **nuclear** and **higher-order processes** in the analysis of the CD data.

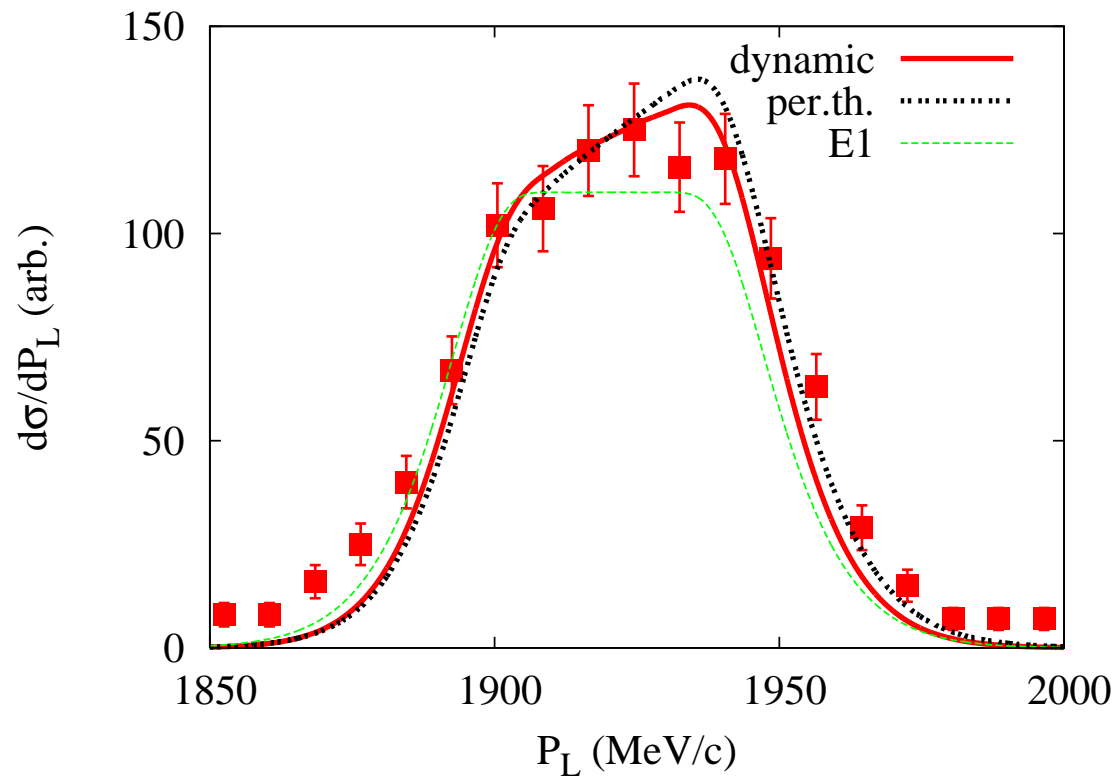


Evidence of E2 transitions in the dissociation of ^8B .

The asymmetry of the LMD of ^7Be fragments is caused by the interference of E1 and E2 transitions.

Esbensen & Bertsch, NPA 600, 37 (1996).

$^8\text{B} \rightarrow ^7\text{Be}$ on Au
at 40 MeV/u.



The asymmetry is reduced by higher-order processes.

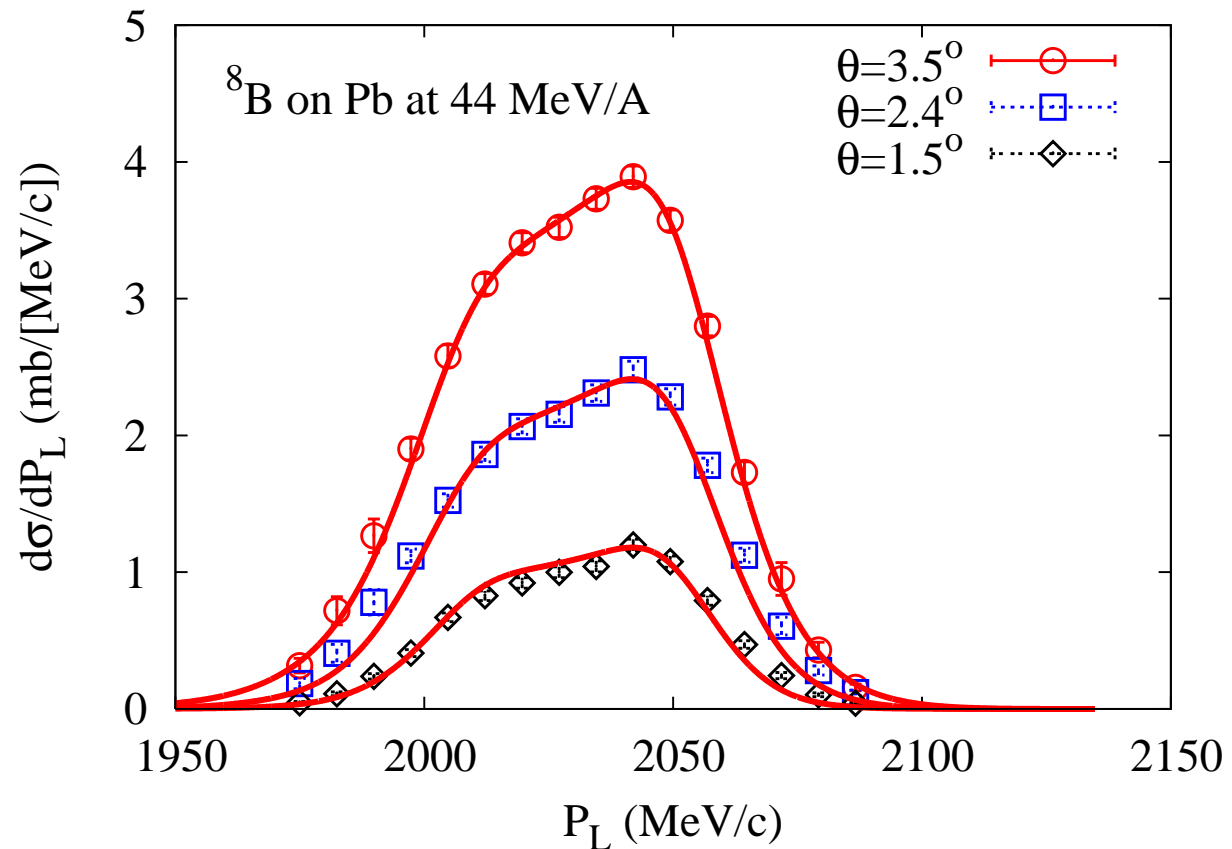
Experiment by *Kelley et al.*, PRL 77, 5020 (1996).

LMD of ${}^7\text{Be}$ fragments

in the Coulomb dissociation of ${}^8\text{B}$ at 44 MeV/A on Pb.

Best fit:

$$d\sigma/dP_L = 1.22 \times |E1 + 0.7 * E2|^2.$$



MSU experiment by *B. Davids et al.*, PRL 81, 2209 (1998).

The reduction in the necessary E2 strength, $|0.7 * E2|^2$, is likely caused by the neglect of higher-order processes.

Dynamic effects and breakdown of far-field approximation.

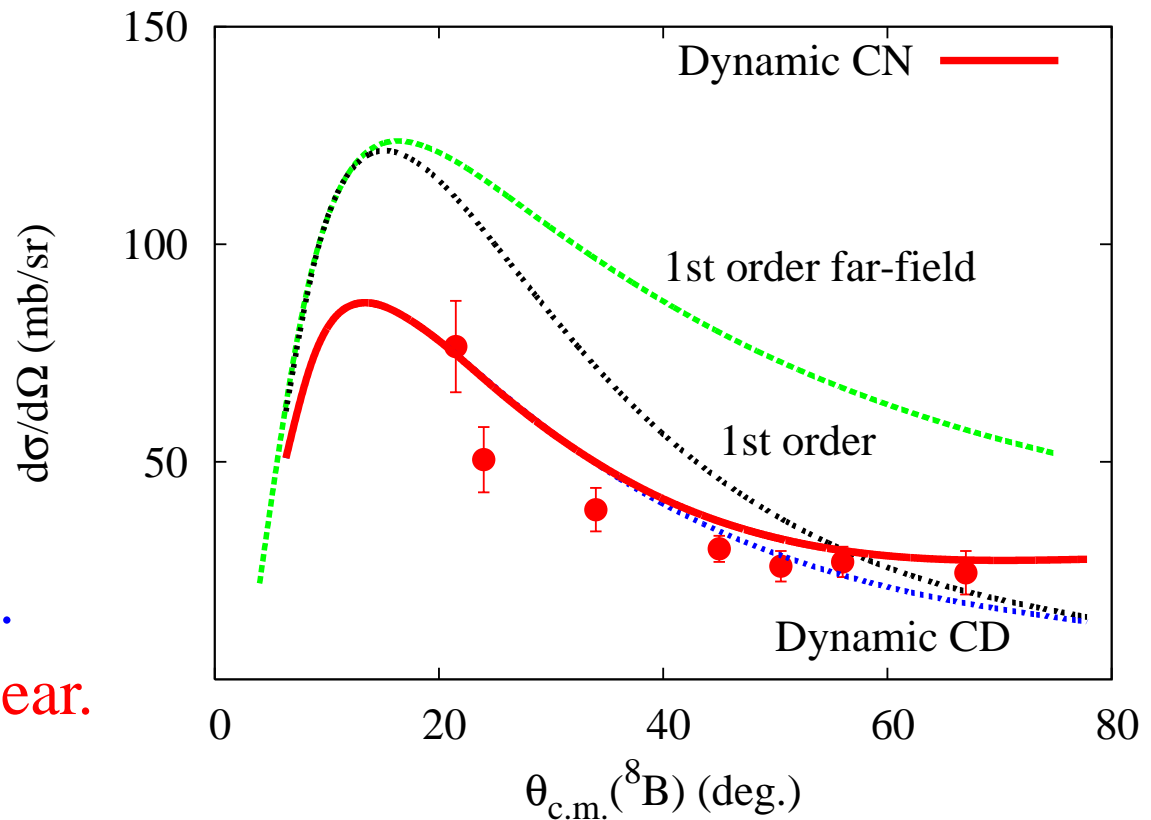
$^8\text{B} \rightarrow ^7\text{Be}$ breakup on Ni at 25.75 MeV at Notre Dame,
Guimarães et al., PRL 84, 1862 (2000).

First-order E1+E2
far-field approximation.

Correct 1st-order
E0+E1+E2
Coulomb dissociation.

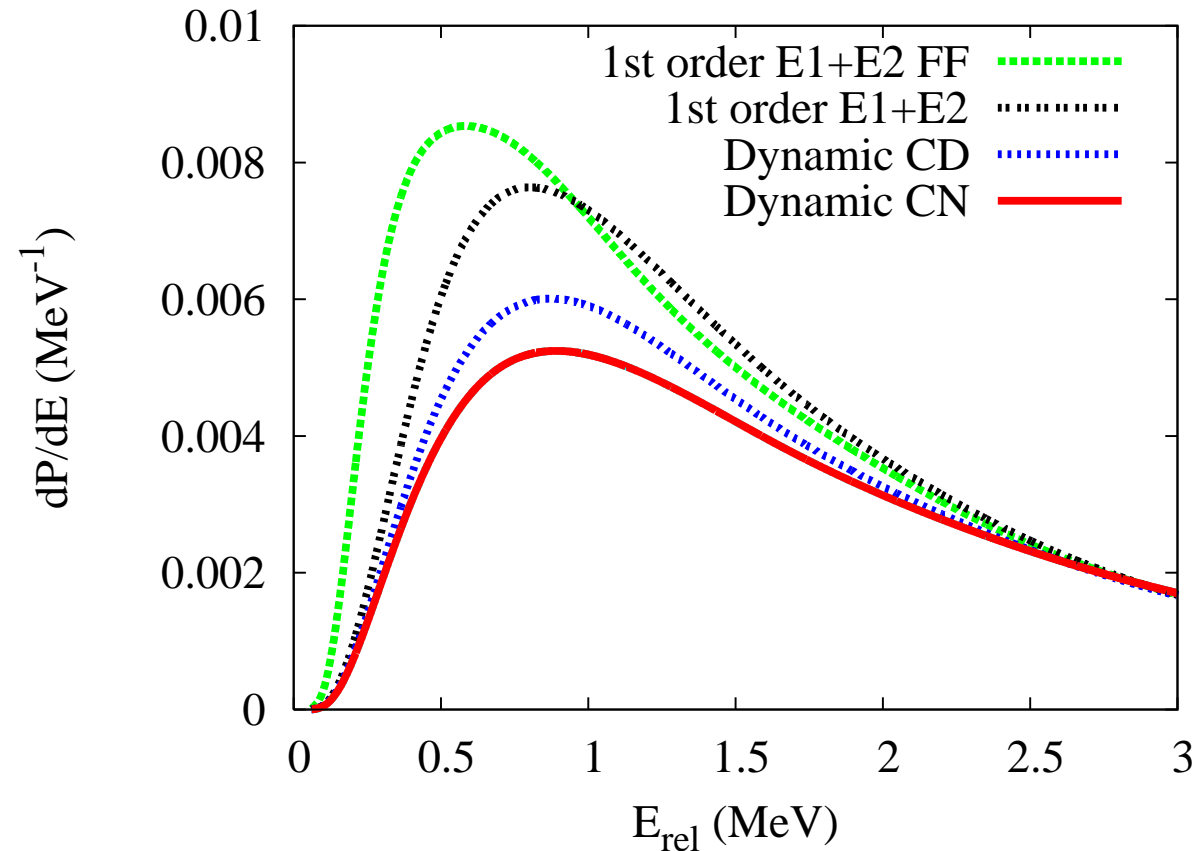
Dynamic Coulomb dissociation.
Dynamic Coulomb + nuclear.

Esbensen and Bertsch,
PRC 66, 044609 (2002)



Effects on the decay energy spectrum, dP/dE_{rel} ,
for ${}^8\text{B} \rightarrow {}^7\text{Be}+p$ on Pb at 52 MeV/u and fixed $b=20$ fm.

Related to RIKEN
experiment by
Kikuchi et al.



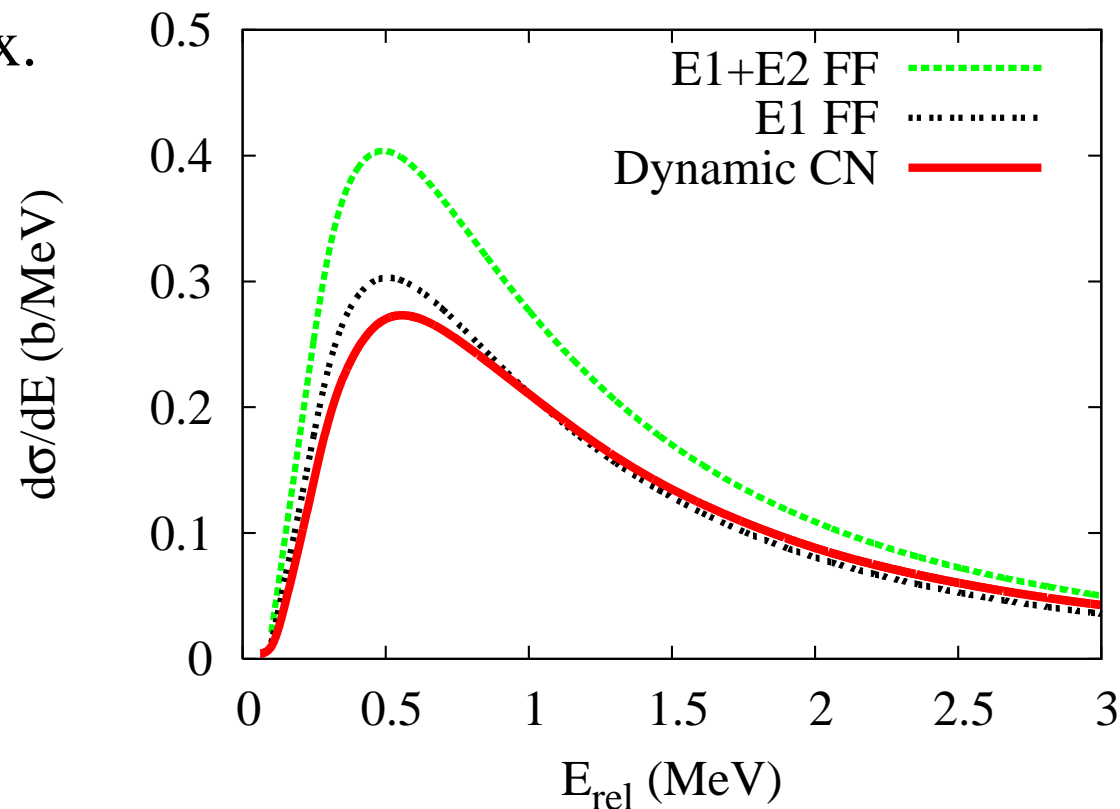
Esbensen, Bertsch & Snover, PRL 94, 042502 (2005).

Calculated decay energy spectra, $d\sigma/dE_{rel}$,
for ${}^8\text{B} \rightarrow {}^7\text{Be}+p$ on Pb at 52 MeV/u.

Esbensen, Bertsch & Snover, PRL 94, 042502 (2005).

FF: Far-Field approx.

$$V_\lambda \propto r_p^\lambda / R^{\lambda+1}.$$



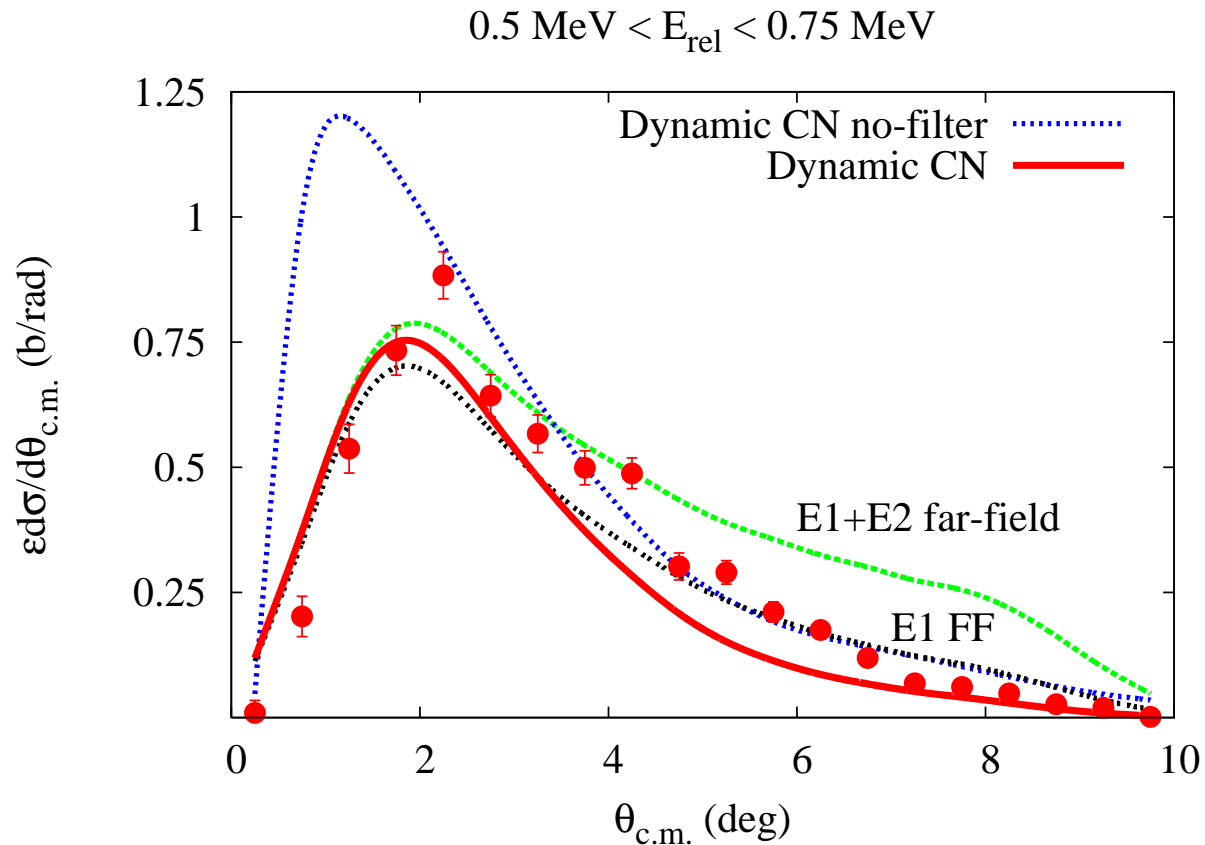
$$V_{pT} = \text{CH89}.$$

$$V_{cT}=0, b_0 = 12 \text{ fm}.$$

The dynamic Coulomb-Nuclear calculation is slightly suppressed compared to the first-order E1 FF approximation.

Analyze data with Dynamic-CN gives a larger $dB(E1)/dE$.

RIKEN experiment: ${}^8\text{B} \rightarrow {}^7\text{Be} + \text{p}$ on Pb at 52 MeV/u.
by *Kikuchi et al.*, PLB 391, 261 (1997).



Best fit: multiply Dynamic CN calculation by 1.17.

Coulomb Dissociation of ^8B versus radiative proton capture on ^7Be .

Coulomb dissociation,

Kikuchi et al. (RIKEN),

PLB 391, 261 (1997):

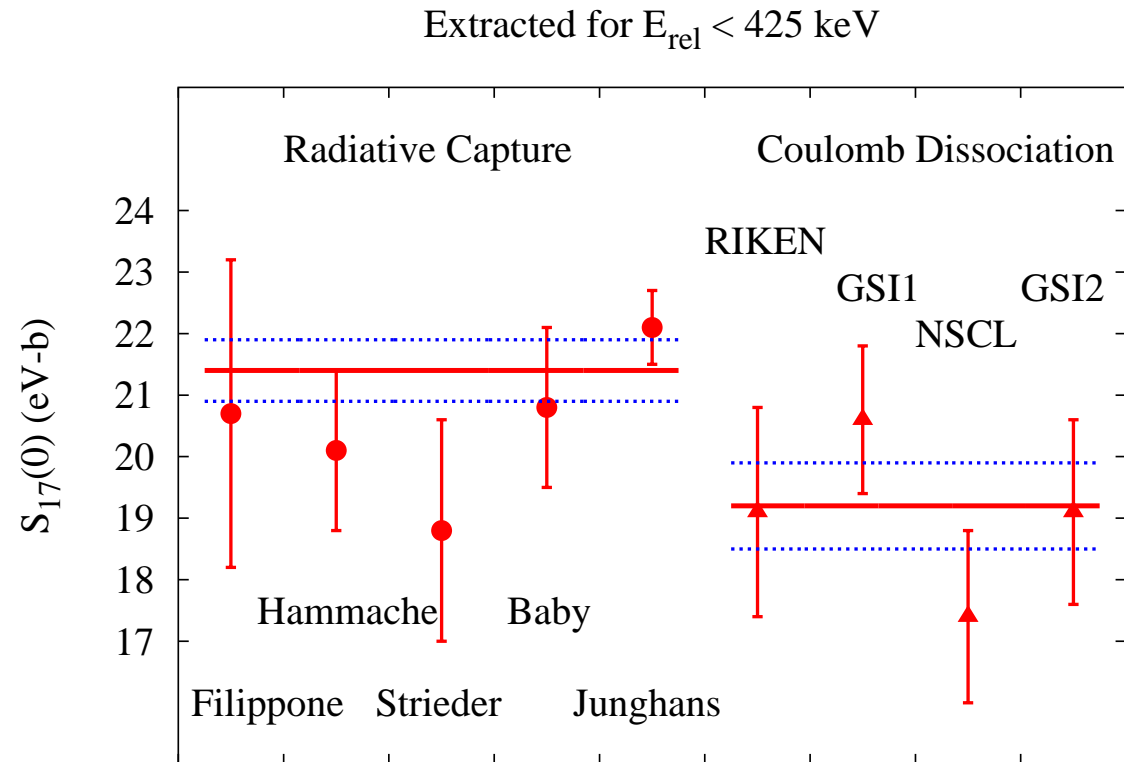
$$S_{17}(0) = 19.1(17) \text{ eV-b.}$$

Radiative proton capture,

Junghans et al. (Seattle),

PRC 68, 065803 (2003):

$$S_{17}(0) = 22.1(6)(7) \text{ eV-b.}$$



A 15% discrepancy. The discrepancy may be due to the break-down of the far-field approximation, the neglect of E2 transitions, higher-order Coulomb and nuclear processes,

Esbensen, Bertsch & Snover, PRL 94, 042502 (2005).

Reconciling **CD** and **RC** measurements.

The discrepancy was resolved by *Ogata et al.*, PRC 73, 024605 (2006), who used the CDCC method to analyze the RIKEN **CD** experiment. They obtained $S_{17}(0) = 20.9(20)$ eV-b, instead of 19.1(17) eV-b.

Junghans et al. PRC 81, 012801 (2010).

Updated value: $S_{17}(0) = 21.5(6)(7)$ eV-b, instead of 22.1(6)(7) eV-b.

Recommended value: $S_{17}(0) = 20.8(16)$ eV-b,

Adelberger et al., RMP 83, 195 (2011).

The ANCs from Variational Monte Carlo calculations predict:

$$S_{17}(0) = 38.7 (A_{p_{1/2}}^2 + A_{p_{3/2}}^2) = 20.8 \text{ eV-b,}$$

Nollett & Wiringa, PRC 83, 041001(R) (2011).

Coulomb dissociation of ^{15}C

$1/2^+$ ground state, $S_n = 1.218$ MeV.

$5/2^+$ excited state at $E_x = 0.74$ MeV.

$3/2^+$ resonance at $E_x = 4.780$ MeV, $\Gamma = 1.740$ MeV.

Simulate the structure of ^{15}C by Woods-Saxon wells.

Table 1: The depth V_l is adjusted for s -, p -, and d - waves.

R (fm)	a (fm)	V_s (MeV)	V_p (MeV)	V_d (MeV)	V_{so} (MeV)
2.946 ^{a)}	0.5 ^{a)}	55.36 ^{a)}	55.36 ^{b)}	52.03 ^{c)}	4.86 ^{c)}

^{a)} Was introduced by *Terry et al.*, PRC 69, 054306 (2004).

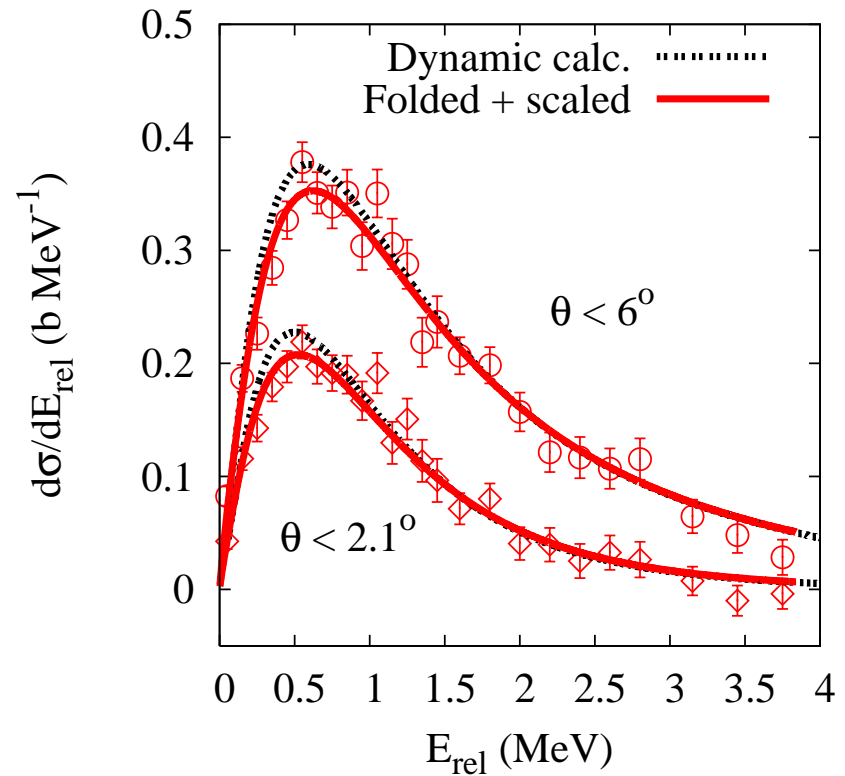
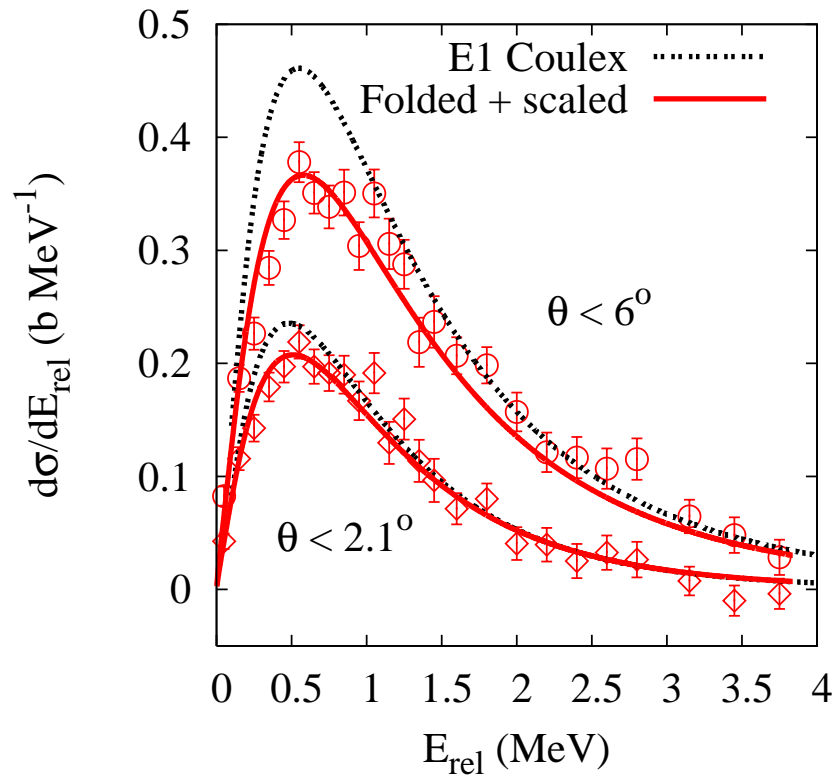
^{b)} *Nakamura et al.*, PRC 79, 035805 (2009) chose $V_p = V_s$ so that *Siegert's* theorem applies to E1 transitions.

^{c)} V_d and V_{so} were adjusted to simulate the $5/2^+$ and $3/2^+$ states.

U_{nT} = Perry-Perry pot. U_{cT} = scaled $^{17}\text{O}+\text{Pb}$ opt. pot. (Fukuda).

$^{15}\text{C} \rightarrow ^{14}\text{C} + n$ dissociation on Pb at 68 MeV/A.

Nakamura et al., PRC 79, 035805 (2009).



Solid curves have been folded with the experimental resolution,
and scaled to give the best fit to the data.

Esbensen, PRC 80, 024608 (2009).

Optimum scaling factors S_c

The best first-order E1 fit to the data requires a scaling by

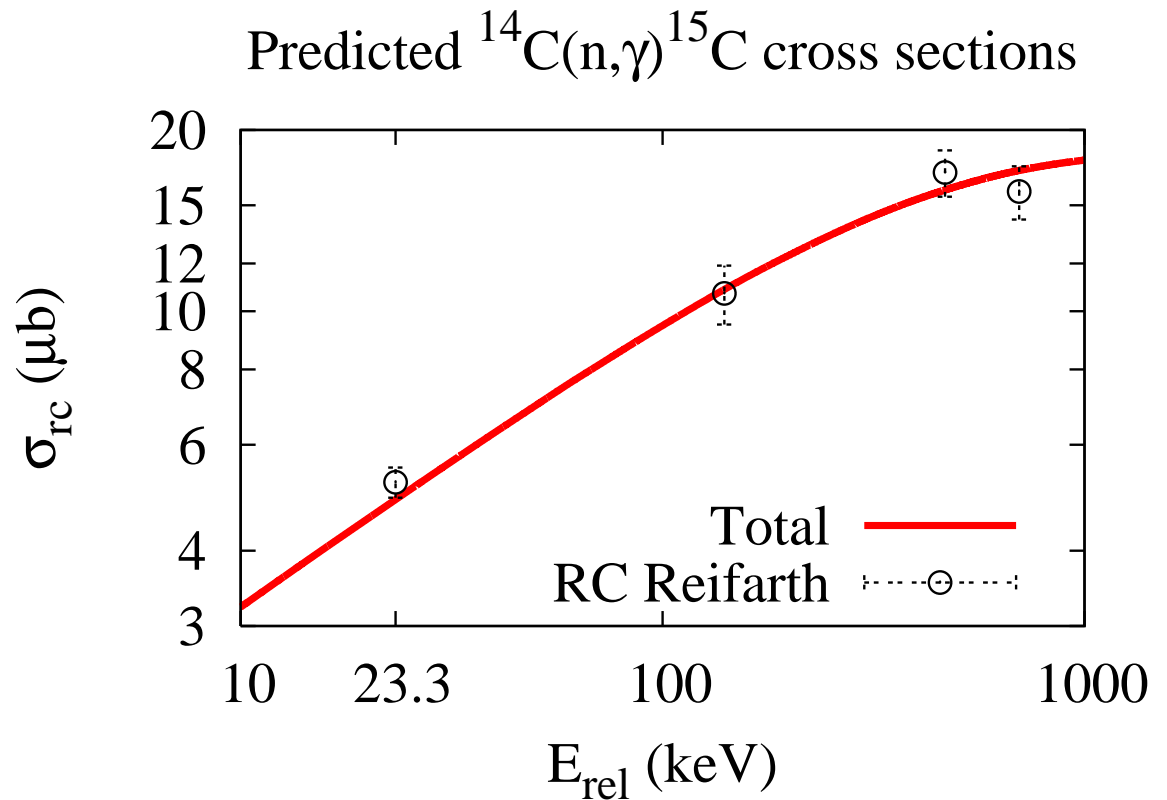
$$S_c = 0.94 \text{ for } \theta < 2.1^\circ,$$
$$S_c = 0.84 \text{ for } \theta < 6.0^\circ.$$

The **dynamic calculation** requires $S_c \approx 0.98$ consistently at both opening angles.

The predicted radiative capture (RC) cross section

includes a 4% contribution from the capture to the $5/2^+$ excited state.

Capture measurement: *Reifarth et al.*, Phys. Rev. C 77, 015804 (2008).



Comparison to the $^{14}\text{C}(n,\gamma)^{15}\text{C}$ experiment by *Reifarth et al.*, Phys. Rev. C 77, 015804 (2008).

Some confusion about the Maxwellian average capture cross section!

They quote the cross section $5.2(3) \mu\text{b}$ at $E_{cm} = 23.3 \text{ keV}$.

That is **10% larger** than the $4.74(34) \mu\text{b}$ I obtain from the analysis of the CD experiment.

A discrepancy of 1σ .

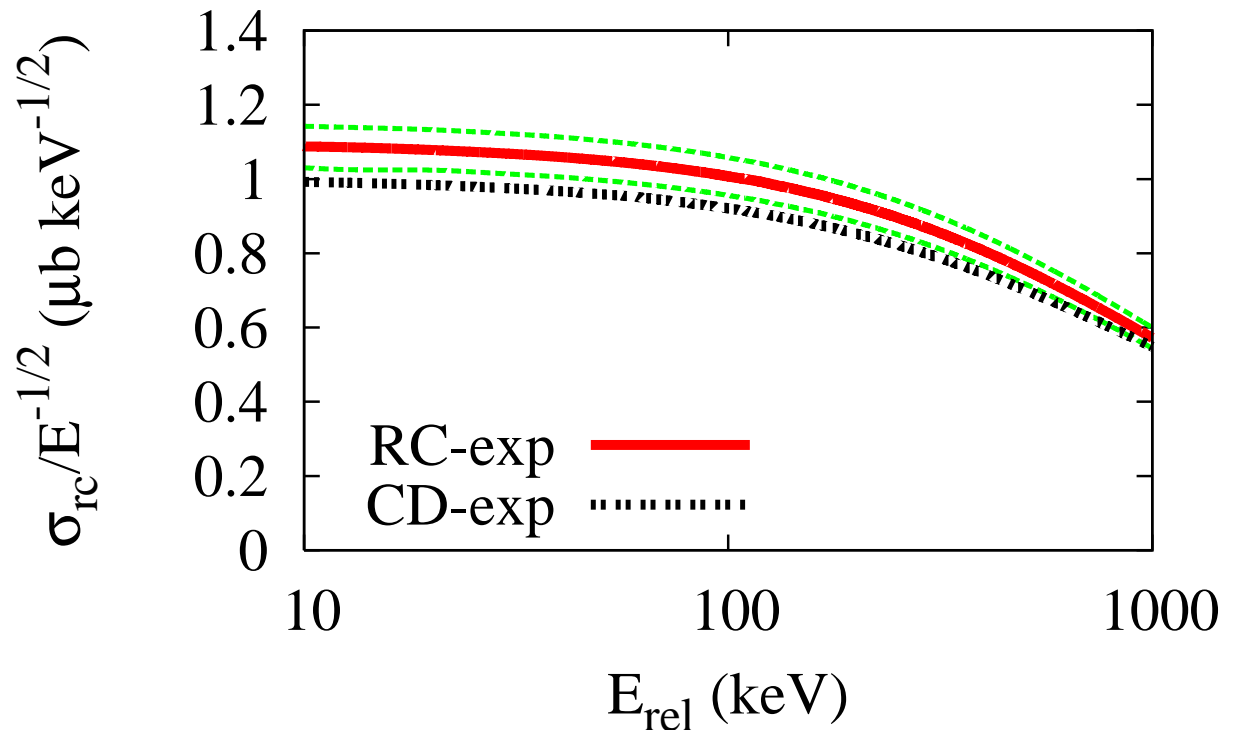
Plot $\sigma_{n\gamma} / \sqrt{E_{cm}}$

Error band on
RC-exp. $\approx \pm 5\%$.

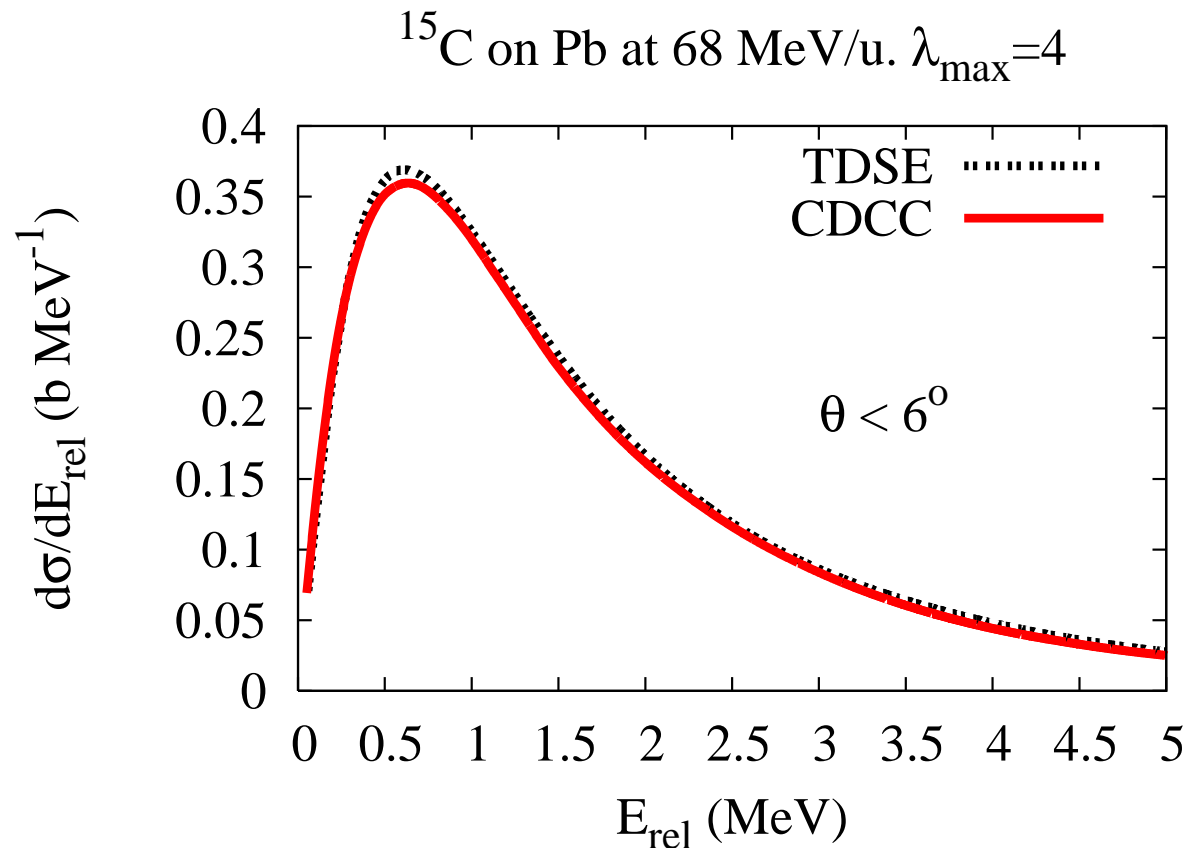
Error band on
CD-exp. $\approx \pm 7\%$.

Esbensen & Reifarth,
Phys. Rev. C 80, 059904 (2009).

$^{14}\text{C}(n,\gamma)^{15}\text{C}$ cross sections



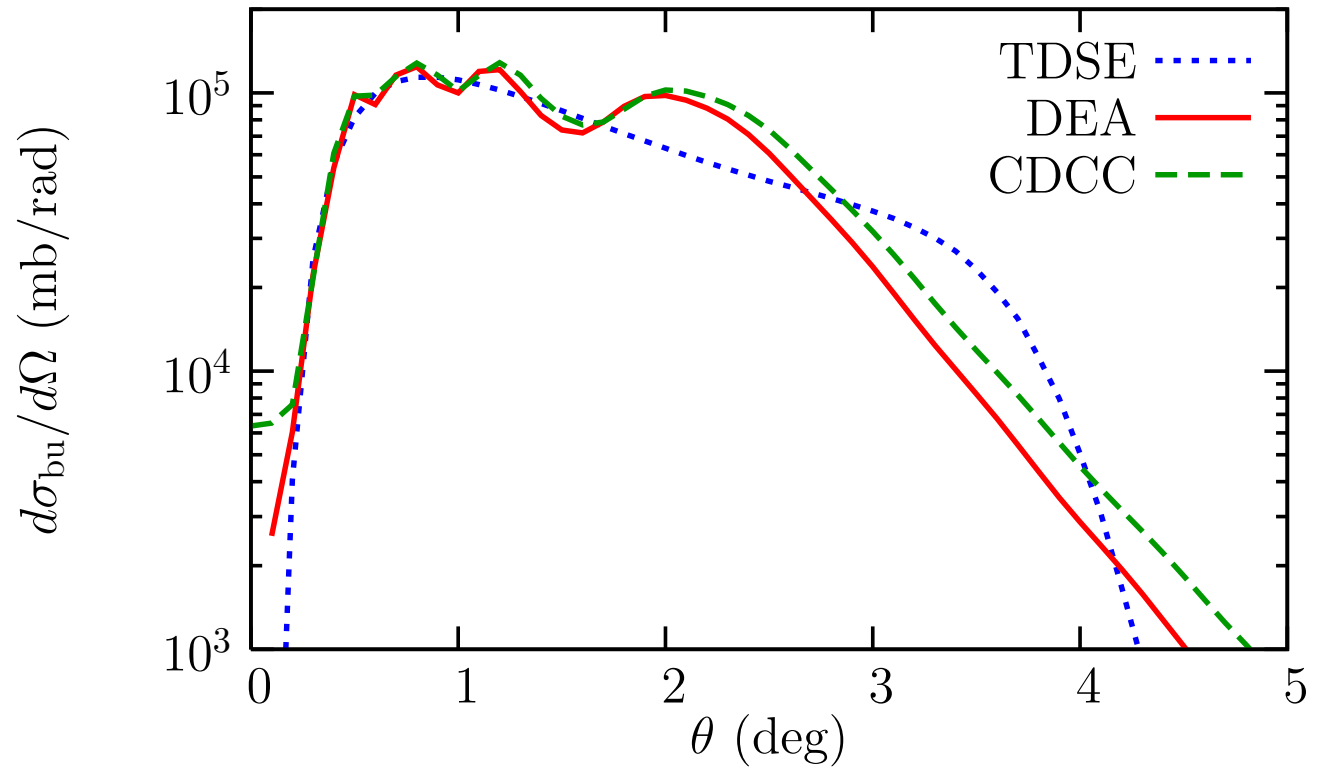
Comparison of the semiclassical (TDSE) method to
Continuum Discretized Coupled Channels (CDCC) calculations.
Capel, Esbensen & Nunes, PRC 85, 044604 (2012).



The peaks of the TDSE and CDCC calculations differ by 2%.

Comparison of angular distributions of the breakup

The semiclassical TDSE calculation does not exhibit any of the quantum interference of the CDCC calculation.



That could be fixed as done in **DEA**, the **Dynamical Eikonal Approximation**, *Baye et al.*, PRL 95, 082502 (2005).

Summary

A collaboration with George, from 1995 - 2005.

- The dissociation of halo nuclei on a high-Z target is a useful tool to determine the rate of the inverse, radiative capture.
- Works well for ^8B when analyzed by CDCC calculations (*Ogata et al.*) - The first-order far-field approximation is inaccurate.
- The semiclassical, dynamic method describes the measured ^{15}C decay energy spectra consistently at small and large angles. The extracted E1 strength is consistent with $^{14}\text{C}(n,\gamma)^{15}\text{C}$ capture data.
- The method agrees very well with CDCC calculations (*Capel et al.*)
 - One should include interference effects in the angular distribution.

Work supported by U.S. Department of Energy,
Office of Nuclear Physics

